Molecular Crystals and Liquid Crystals

Publication details, including instructions for authors and subscription information:
http://www.tandfonline.com/loi/gmcl20

Real-Time Imaging Spectrometry of Tissues for Photodynamic Diagnosis (PDD)

Liming Li [a], Katsuo Aizawa [a] & Fumihiko Ichikawa [b]

[a] Faculty of Photonics Science and Technology, Chitose Institute of Science and Technology, Chitose, Japan

[b] Senior Research Engineer, Technical Service Center, Kawasaki Steel Techno-research Corporation, Chiba, Japan

Version of record first published: 22 Sep 2010

To cite this article: Liming Li, Katsuo Aizawa & Fumihiko Ichikawa (2007): Real-Time Imaging Spectrometry of Tissues for Photodynamic Diagnosis (PDD), Molecular Crystals and Liquid Crystals, 472:1, 343/[733]-352/[742]

To link to this article: http://dx.doi.org/10.1080/15421400701548696

Mol. Cryst. Liq. Cryst., Vol. 472, pp. 343/[733]–352/[742], 2007

ISSN: 1542-1406 print/1563-5287 online
DOI: 10.1080/15421400701548696

Taylor & Francis
Taylor & Francis Group

Real-Time Imaging Spectrometry of Tissues for Photodynamic Diagnosis (PDD)

Liming Li
Katsuo Aizawa
Faculty of Photonics Science and Technology, Chitose Institute of Science and Technology, Chitose, Japan

Fumihiko Ichikawa
Senior Research Engineer, Technical Service Center, Kawasaki Steel Techno-research Corporation, Chiba, Japan

A novel imaging spectrometry was demonstrated which can accurately measure the spectrum of whole surface of tissue instead of a single point. Using this apparatus, we obtained the microscope spectrometry image of the hematoxylin-eosin stained tumorous tissue and normal (muscle and blood vessel) mouse tissue was obtained. From the pseudo RGB images of the spectra, tumorous and normal tissues were observed very clearly. The spectra at arbitrary positions could be taken instantly as well as the transmission and absorption spectra, which normalized to the background spectrum. The spectral intensity distribution images were obtained at selected wavelengths to get the area distribution of the stained tumorous and normal tissue clearly. In our experiments, we obtained clear spectrometry imaging from weakly illuminated objects. It took 30 seconds to measure a static image of a sample. Moreover, this apparatus is suitable for real-time measurements of living tissue if using laser illumination, a high-speed CCD camera, a fiber, an endoscope and photosensitizer. In the near future, this novel technique can be used in tumor photodynamic diagnosis.

Keywords: hematoxylin-eosin; imaging spectrometry; malignant tumor; microscope; photodynamic diagnosis; RGB imaging; spectral intensity; spectral intensity distribution images; tissue screening; transmittance

Address correspondence to Liming Li, Faculty of Photonics Science and Technology, Chitose Institute of Science and Technology, 758-65 Bibi, Chitose, Hokkaido 066-8655, Japan. E-mail: liliming@photon.chitose.ac.jp

1. INTRODUCTION

Now the main method of malignant tumors diagnosis is using endoscopes to observe the tissue by naked eye then sample of the suspected focus tissue to make pathologic analyses on the cell. However this method will not only increase the pain of the patient, but also increase the risk of dispersing the tumor cells. So the people hope to use imaging spectrometry for early malignant tumor diagnosis instead of sampling the tissue cells.

Significant research attention has been focused on the photodynamic diagnosis (PDD) technique, which combines a photosensitizer and a specific excitation wavelength. Because of negligible side effects, the ability to find and diagnose tumorous tissue is possible. PDD autofluorescence uses a laser to excite the fluorescence material porphyrin inside the tumor and to measure the fluorescence spectrum for tumor diagnosis [1–3]. PDD fluorescence, however, utilizes injected photosensitizer. The photosensitizer accumulated in tumor then excited the tissue using a laser which generates fluorescence [4–7]. Small tumorous tissue and its position also can then be diagnosed accordingly. Both techniques are dependent on the imaging spectrometry to analyze images and spectra.

Up to now, the fluorescence spectrum of only one point in the image could be measured by imaging spectrometry [8,9]. It was difficult to obtain a relationship between the exact position and the spectrum. The information based on fluorescence spectrum of one point was not sufficient for proper diagnosis. In order to overcome these shortcomings, we constructed an instrument [10–12] that can instantaneously measure the position and spectra of multiple points in human tissue. As an attempt of the new real-time imaging spectrometry method, we measured the microscope real-time spectrometry image of tumorous and normal (muscle and blood vessel) tissue of mice as a pathological sample.

2. MATERIALS AND METHODS

2.1. Real-Time Image Spectrometry System

The schematic of the real-time imaging spectrometry system is shown in Figure 1. The light from a line A–B on the sample passes through a slit and a transmission grating, housed within an imaging spectrometer (Imspector made by Imaging Led. Company), is displayed on a single frame and recorded by a CCD camera (Fig. 2, spectra range: 380–780 of Line A–B, length is in nm, and wavelength

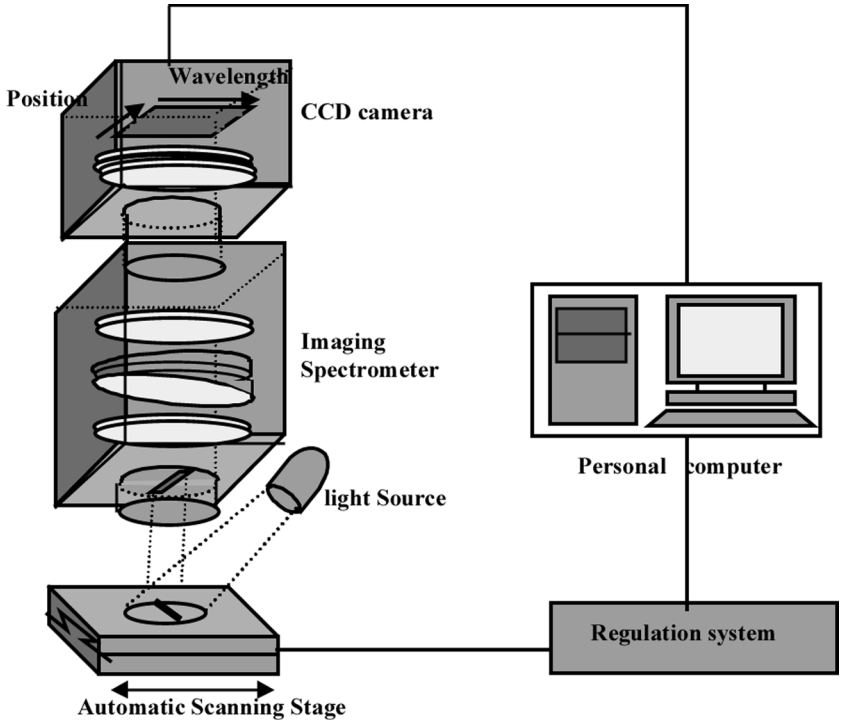

FIGURE 1 The Schematic diagram of the high sensitivity imaging spectrometry system. Light source, halogen lamp; Imaging spectrometer, wavelength range 380–780 nm, wavelength resolution 2 nm; updated time 0.1–2.1 sec/line; CCD image intensifier, wavelength range 380–850 nm, sensitive 20 μ Lux.

resolution is 2 nm). The data from the CCD image are the distributions of wavelength (on the Y-axis) as a function of spatial position, X. A two-dimensional spatial image is recorded when the sample stage is driven by a computer-controlled motor (measures time: 0.1–2.1 sec/line, 30 sec/frame).

The spectra image is recorded by monochrome camera with an image intensifier (luminance gain: 2500, sensitivity: 20 μ lux, wavelength range: 380–850 nm, and wavelength resolution: 2 nm). It can be used to measure a single line of spectrum. After processing the position information in the computer, we can obtain the RGB color values x, y, z, R, G, B from the spectral intensity every 5 nm and display the RGB pseudo color image. Then it can display the spectrum for a single point or a pair of points and its differential data, direct data,

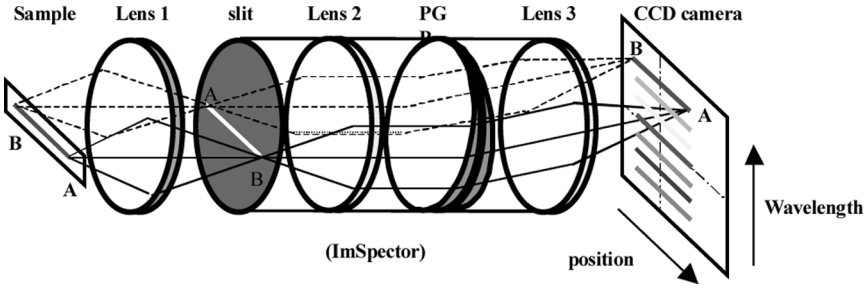

FIGURE 2 Principle of imaging spectrometry.

reflectivity (transmission ratio). It also can show the monochrome intensity resolution for any spectral wavelength.

2.2. Sample Preparation and the Observation of the Microscope Real-Time Imaging Spectrometry

Type BALB/C male mice, 5 weeks of age were used in this animal experiment. 1×10^6 Meth-A fibrosarcoma cells were transferred to right thigh tissue subcutaneously. Then a 1-cm-diameter tumor was formed after a week. The mice were anesthetized to death for dissection. The tumorous and normal tissue was taken out, fixed by 10% neutral formalin. Both the tumorous and normal tissue was sliced into thin samples and stained by hematoxylin-eosin. The samples were placed on the stage and observed by 10-times magnification microscope. The real-time spectrometry images were observed with the stage being driven at 1 mm/min, which is synchronized with the CCD camera.

3. RESULTS AND DISCUSSION

3.1. Observation on the Real-Time Spectrometry Imaging of Mice Malignant Tumor Tissue

3.1.1. RGB Imaging of Mice Malignant Tumor Tissue

The malignant tumorous mouse tissue stained by hematoxylin-eosin was measured by imaging spectrometry. Figure 3 is the image of entire tumor tissue shown by pseudo color (RGB), in which the RGB are calculated from the spectral intensity. The figure is nearly identical with the one captured by color camera.

3.1.2. Spectral Intensity and Transmission

The instantaneous absorption spectra of location A–E, which indicated in Figure 3, are shown in Figure 4(a). It is derived from the imaging

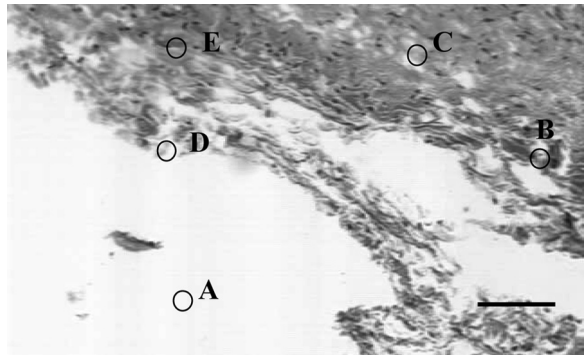

FIGURE 3 RGB imaging of the mice tumor tissue stained by hematoxylin-eosin. The scale bar is 50 um.

spectrometry recorded in our instrument. A is the background there is no tissue existed so no hematoxylin-eosin can be find. The curve of location A in the spectra of Figures 4(a) and (b), there is no absorption peak of eosin can been found. In the Figure 3, the location B is the deep eosin stain portion of the cytoplasm, and the location C is the shallow eosin stain part of the cytoplasm where the cytoplasm is degradation. In the Figure 4, the absorption and transmission peaks and shoulders of curve B and C are observed at 535 nm and 500 nm respectively, just as in eosin. From the Figure 3, the location D is the orange stain surrounded the tissue because of the red cell exist. In Figure 4, the spectrum of the orange part, D, also exhibit a peak as in eosin but

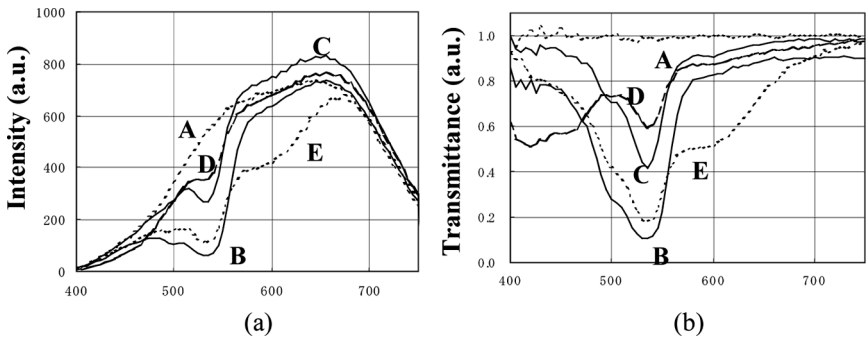

FIGURE 4 The absorption and transmission spectra for locations A–E as marked in Figure 3. (a) The measured absorption spectrum at selecting points (b) The normalized transmission rate at selecting points.

has an additional peak at 420–460 nm. It is come from hemoglobin. E is the hematoxylin-eosin stain part of the cytoblast. The absorption and normalized transmission spectra of marked by E has a peak at 535 nm and a shoulder at 500 nm just as eosin. However, there is an additional shoulder at 560–600 nm.

The spectral intensity near 400 nm is very weak because a halogen lamp was used for illumination. Figure 4(b) is the transmission ratio of B, C, D calculated on the basic assumption that the transmission ratio for A is 1.

3.1.3. Spectral Intensity Distribution Images

Figure 5 shows the image of selected wavelengths derived from imaging spectrometry: (a) 425 nm, (b) 505 nm, (c) 535 nm, and (d) 600 nm. The deep color part around the tissue can be clearly displayed in the image at 425 nm. It coincides well with the absorption peak at 420–460 nm of the orange part shown in Figure 5a. The eosin stained part of cytoplasm is clearly displayed in the image at 505 nm and 535 nm shown in Figures 5(b) and (c). The cytoblast is shown clearly in the image at 600 nm (Fig. 5(d)), which is confirmed by the absorption at 500–600 nm of the hematoxylin-eosin stained part. Compare Figure 3 with Figure 5, it was found that the distribution of the stained

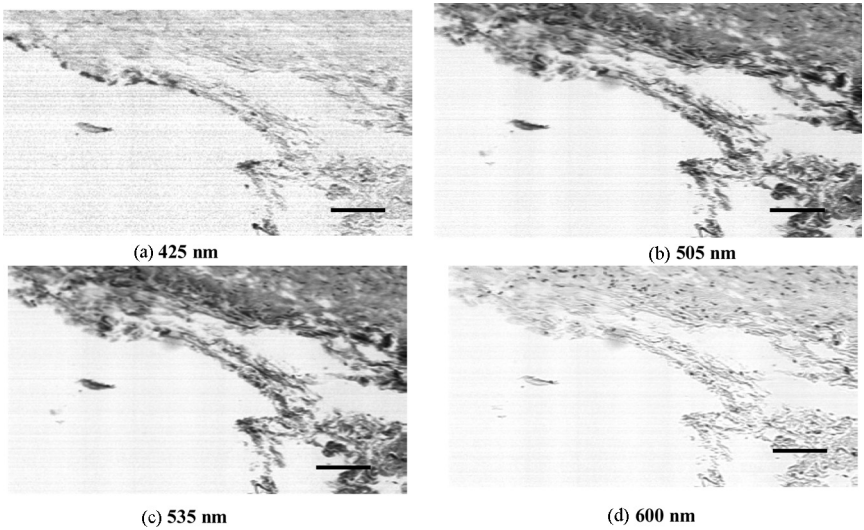

FIGURE 5 The images at selected wavelengths of the stained mice tumor tissue. The scale bars are 50 um.

material can be appeared more clearly if suitable wavelength was selected based on certain images.

3.2. Observation on the Real-Time Spectrometry Imaging of Mice Normal Tissue

3.2.1. RGB Imaging of Mice Normal Tissue

Figure 6 shows the RGB image of normal mouse tissue stained by hematoxylin-eosin. It was measured by imaging spectrometry. This pseudo-color RGB image corresponds to the spectral intensity. The image is different with the tumorous tissue obviously (see Fig. 3), that the muscle and the blood vessel can be seen clearly.

3.2.2. Spectral Intensity and Transmission

Figure 7(a) is the absorption spectra of the positions (A–D) in Figure 6. The location A is the non-tissue part of vessel wall. B is the deep eosin stain part of muscle cytoplasm. C is the red blood cell in the blood vessel. Finally, D is the hematoxylin-eosin stain part of the cytoplast and nuclei.

Figure 7(b) is the normalized transmission rate of Figure 7(a). In the absorption spectra (from 500 to 560 nm) of the eosin stained part of cytoplasm B, a peak and a shoulder are observed at 545 nm and 520 nm, respectively. In general, the shoulder at 520 nm is much weaker than the peak 545 nm. But for the muscle, the shoulder

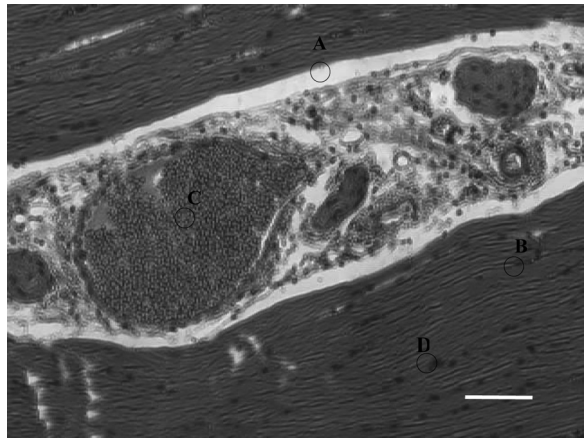

FIGURE 6 RGB imaging of normal mice tissue stained by hematoxylin-eosin. The scale bar is 50 um.

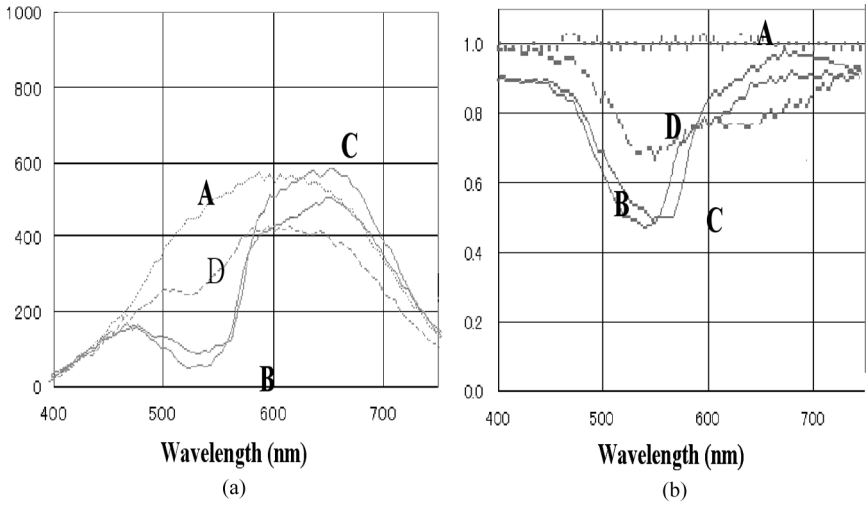

FIGURE 7 The spectra for locations A–E as marked in Figure 6. (a) The measured absorption spectra. (b) The normalized transmission spectra.

became larger due to the overlap with the absorption wavelength of the myoglobin. There is a peak in the absorption spectra (from 520 nm to 570 nm) of the red blood cell C at 555 nm. Normally, after the hemoglobin combines with oxygen, the absorption spectra has two peaks at 540 and 577 nm, while the deoxidize hemoglobin has only one peak at 555 nm. In our experiment, there is a peak at 555 nm in the spectra of the mouse blood vessels stained by hematoxylin-eosin. We can observe a peak at 550 nm in the absorption spectra (from 520 to 650 nm) of D stained by hematoxylin-eosin, and a shoulder at 640 nm, which is unique to hematoxylin-eosin.

3.2.3. Spectral Intensity Distribution Images

We can derive the Figure 8 at a selected wavelength (a: 450 nm, b: 550 nm, c: 570 nm, d: 595 nm) from the imaging spectrometry of normal tissue. If the selected wavelength is within the absorption of the part B–D, we can obtain the intensity distributions corresponding to B–D. For example, at 550 nm on the Figure 8(b) is the muscle distribution, and at 570 nm, Figure 8(c) is the red blood cell distribution in blood vessel. At 595 nm, the cytoblast is shown in Figure 8(d). If the selected wavelength is at the absorption peak of red blood cell, the red blood cell in the Figure 8(b) appear block. If the selected wavelength is not located within the absorption region of red blood cell

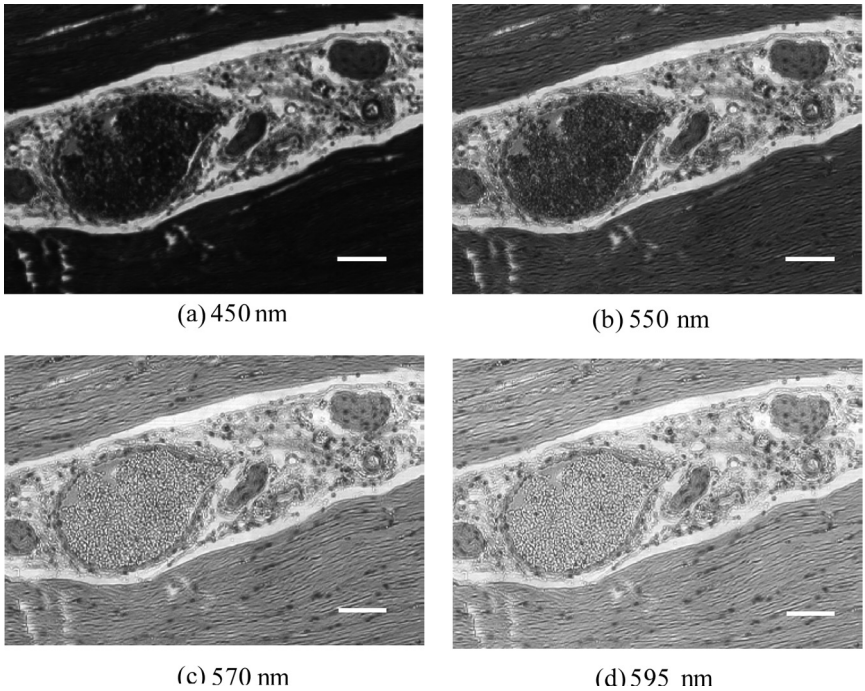

FIGURE 8 The images at selected wavelengths of the stained normal mice tissue. The scale bars are 50 um.

the red blood cell in the image Figure 8(a) is transparent. Therefore we can identify the red blood cell from the identify distribution by selected wavelengths.

4. CONCLUSION

In this article, we demonstrate a novel imaging spectrometry, which can accurately measure the entire tissue surface instead of a single point. Using this apparatus, we took the microscope spectrometry images of the hematoxylin-eosin stained tumorous tissue samples of mice. From the spectra, the calculated RGB images of tumorous tissue were very clear. The spectral intensity distribution image was also obtained at selected wavelengths in order to properly identify the tissue components, for the purpose of using this instrument in diagnostic tissue screening. In our experiments, we obtained clear spectrometry imaging from weakly illuminated objects. It took 30 seconds to obtain a static image of a sample. Moreover, this apparatus is

suitable for real-time measurements of living tissue if using laser illumination, a high-speed CCD camera, a fiber, an endoscope, and photosensitizer. In the near future, this novel technique can be used in tumor photodynamic diagnosis.

REFERENCES

[1] Li, L., Yie, Y., & Yang, Y. (1991). Laser excited malignancy autofluorescence for tumour malignancy detection, Proceedings of World Congress on Medical Physics and Biomedical Engineering, p. 849.
[2] Yang, Y., Li, L., & Yie, Y. (1990). Laser excited autofluorescence for brain tumour and accumulation of endogenous porphyrin. *Chinese Journal Lasers*, *17*(5), 318–321.
[3] Yang, Y., Yie, Y., & Li, L. (1990). A study on autofluorescence of transplanted cancer in rats and mice. *Chinese Journal Lasers*, *17*(1), 61–63.
[4] Pandey, R. K., Majchrzycki, D. F., Smith, K. M., & Dougherty, T. J. (1989). Chemistry of photofrin II and some new photosensitizers. *Proc. SPIE*, *1065*, 164–174.
[5] Tsuchida, T., Aizawa, K., Konaka, C., & Kato, H. (1993). Interaction of bovine serum albumin with mono-L-aspartyl chlorin e6 by Spectrophotometry. *Lasers in the Life Sciences*, *5*(3), 155–164.
[6] Sheyhedin, I., Okunaka, T., Kato, T., Yamamoto, Y., Sakaniwa, N., Konaka, C., & Aizawa, K. (2000). Localization of experimental submucosal esophageal tumor in rabbits by using Mono-L-aspartyl chlorin e6 and long-wavelength photodynamic excitation. *Laser Surg. Med.*, *26*(19), 83–89.
[7] Li, L., Aizawa, K., Kodama, K., & Minamitani, H. (2001). Accumulation to malignant tumor of pheophorbide derivative PH-1126 for photodynamic diagnosis studied in vivo. *Bioimages*, *9*(3–4), 170–116.
[8] Kato, H., Aizawa, K., Ono, J., Konaka, C., Kawate, N., Yoneyama, K., Nishimiya, K., Sakai, H., Noguchi, M., Tomono, T., Kawasaki, S., Tokuda, Y., & Hayata, Y. (1984). Clinical measurement of tumor fluorescence using a new diagnostic system with hematoporphyrin derivative laser Photoradiation and spectroscope. *Laser Surg. Med.*, *4*, 49–58.
[9] Hirano, T., Ishizuka, M., Suzuki, K., Ishida, K., Suzuki, S., Miyaki, S., Honma, A., Suzuki, M., Aizawa, K., Kato, H., & Hayata, Y. (1989). Photodynamic cancer diagnosis and treatment system consisting of pulse lasers and an endoscopic spectro-image analyzer. *Lasers in the Life Sciences*, *3*(2), 99–116.
[10] Esko, H. & Jukka, O. (1996). Imaging spectrograph and camera solutions for industrial applications. *International Journal of Pattern Recognition and Artificial Intelligence*, *10*(1), 43–54.
[11] Tapio, V., Mauri, A., & Heimo, K. (1997). An advanced prism-grating-prism imaging spectrograph in on-line industrial applications. *SPIE*, *3101*, 322–330.
[12] Timo, H., Esko, H., & Alberto, D. A. (1998). Direct sight imaging spectrograph: a unique add-on component brings spectral imaging to industrial applications. *SPIE Symposium on Electronic Imaging*, *3302*, 165–175.